Struct Chem (2010) 21:955–964
DOI 10.1007/s11224-010-9632-8

ORIGINAL RESEARCH

Synthesis and structural characterization of novel 2-benzimidazolylthioureas: adducts of natural isothiocyanates and 2-amino-1-methylbenzimidazole

Anna Śmiechowska · Witold Przychodzeń · Jarosław Chojnacki · Piotr Bruździak · Jacek Namieśnik · Agnieszka Bartoszek

Received: 3 February 2010 / Accepted: 26 May 2010 / Published online: 17 June 2010
© Springer Science+Business Media, LLC 2010

Abstract Adducts of natural allyl, phenethyl, and benzyl isothiocyanates and 2-amino-1-methylbenzimidazole were synthesized. After optimization of the reaction conditions, the target 2-benzimidazolylthioureas were obtained in reasonable yields. The detailed molecular and crystal structures of these compounds were characterized by spectroscopic and X-ray methods. Spectral analysis demonstrated that *N*-(1-methylbenzimidazolyl)-*N*′-allylthiourea, *N*-(1-methylbenzimidazolyl)-*N*′-benzylthiourea, and *N*-(1-methylbenzimidazolyl)-*N*′-phenethylthiourea exist in solution in an unprecedented three tautomeric forms, whose structures were corroborated unambiguously.

Keywords Thioureas · Isothiocyanates · 2-Aminobenzimidazole · Tautomerism

Introduction

Isothiocyanates (ITCs) are reactive electrophilic agents [1] capable of modifying proteins and other biologically important molecules. Whereas, 2-amino-1-methylbenzimidazole **1** (MABI) is an interesting compound because the structure of the benzimidazole unit is a constituent of various important molecules like vitamin B12 [2]. The reaction between heterocycles containing an exocyclic amino group and ITCs yields unsymmetrical thioureas, which are significant biologically active products [3], modern catalysts in organic synthesis, [4], selective neutral receptors for inorganic anion recognition [5–7], as well as valuable building blocks [8] for self-assembled diverse hydrogen-bonded networks in the solid state and in solution. Therefore, it is crucial to determine the exact molecular and supramolecular structure of unsymmetrical thioureas if we are to design them rationally and to understand their activity and selectivity in the reactions they catalyze.

Until now, only one report has been published of the reaction between **1** and phenylisothiocyanate (PITC). On the basis of X-ray crystallographic data and NMR spectra, Morkovnik [9] claimed that the thus obtained *N*-(1-methylbenzimidazolyl)-*N*′-phenylthiourea adopts only one 1,3-dihydrobenzimidazolinylidene tautomeric form in crystals and in solution. Quantum-chemical calculations (DFT, B3LYP/6-31G**) have confirmed that this sole tautomer has the lowest energy.

In this work, we present an optimized procedure for the conversion of natural ITC to 2-benzimidazolylthioureas **2a–c** (Scheme 1), as well as the results of a study of the structure of their isomers in solution and in crystals. DFT calculations were conducted to rationalize the unusual existence of **2** in three tautomeric forms in solution.

Experimental section

Methods

All reagents (AITC, BITC, PEITC, and **1**) and solvents were purchased from the Aldrich Chemical Company. Solvents were purified and dried using standard procedures.

Electronic supplementary material The online version of this article (doi:10.1007/s11224-010-9632-8) contains supplementary material, which is available to authorized users.

A. Śmiechowska (✉) · W. Przychodzeń · J. Chojnacki · P. Bruździak · J. Namieśnik · A. Bartoszek
Chemical Faculty, Gdańsk University of Technology, ul. Narutowicza 11/12, 80-233 Gdansk, Poland
e-mail: anna_smiechowska@o2.pl

Scheme 1 Synthesis of thioureas **2a**–**2d** and **2e**—derivatives of **1** and 2-amino-*N*-(2-phenoxyethyl)benzimidazole **1′**, respectively (compounds **2d** and **2e** were prepared by Morkovnik [9])

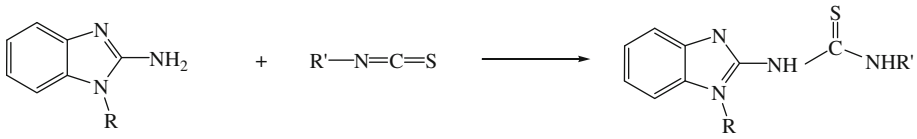

1 R = CH_3
1' R = CH_2CH_2OPh

2a R = CH_3, R' = $CH_2CH{=}CH_2$
2b R = CH_3, R' = CH_2Ph
2c R = CH_3, R' = CH_2CH_2Ph
2d R = CH_3, R' = Ph
2e R = CH_2CH_2OPh, R' = Ph

The course of reaction and homogeneity of the products was monitored by TLC using Merck silica gel plates (60F-254) and the hexane/ethyl acetate (7:3) solvent system.

^1H, ^{13}C, and ^{15}N NMR spectra were recorded at 298 K on a Varian Unity 500 Plus spectrometer in $CDCl_3$ and DMSO-d_6. 1D NOE and ROESY experiments were performed using Varian standard pulse sequences.

The UV–Vis spectra ($CHCl_3$ and CH_3CN solution) were obtained with the aid of a Thermo Scientific NanoDrop 2000c spectrophotometer working under Thermo SCIENTIFIC software.

Elemental analysis for carbon, hydrogen, nitrogen, and sulfur was performed on a CHNS-Carlo Erba EA-1108 Analyzer.

Mass spectra were obtained using a 4000 Q TRAP hybrid triple quadrupole linear ion trap mass spectrometer (Applied Biosystems/MDS Sciex).

ATR spectra of crystals (crystallized substances) were recorded on a Nicolet 8700 spectrometer (Thermo Electron Co.) operating under OMNIC software. ATR spectra were recorded using the Golden Gate ATR accessory (Specac) equipped with a single-reflection diamond crystal. The temperature during measurements was kept at 25 ± 0.1 °C using an electronic temperature controller (Specac). For each spectrum, 64 scans were collected with a resolution of 4 cm^{-1}.

Recrystallization from ethyl acetate–cyclohexane (1:1) using slow cooling of the saturated solution technique afforded single crystals of **2** suitable for X-ray analysis. The experimental diffraction data were collected on a KM4CCD (Oxford Diffraction, now part of Varian) kappa-geometry diffractometer equipped with a Sapphire-2 area detector. An enhanced X-ray Mo Kα radiation source with a graphite monochromator was used. The data reduction was conducted using CrysAlis software package [10]. Structure solution and final refinement were carried out using the SHELX-97 program package [11]. Packing diagrams were prepared using Mercury visualization software [12].

The merging of reflections for compound **2a** (CCDC 751508) was omitted due to technical reasons. Crystals of **2a** turned out to be rotational twins. The twinning was resolved by software at the data reduction stage (the HKLF 5 file was produced), which gave excess of reflections above the number expected for a non-twinned crystal. Selected twinning details: twin matrix [0.9987 −0.0040 −0.0007 −0.6223 −0.9986 −0.0019 −0.9401 0.0054 −0.9977], components ratio 0.4106/0.5894, isolated reflns 3243/3238, overlapped 1721.

All calculations using density functional theory (DFT) were carried out using Gaussian 03 program [13].

Synthetic procedure

A single portion of ITC (6.79 mmole) was added to a solution of **1** (1 g, 6.79 mmole) in MeCN (5 mL). After being stirred for 2 h (for AITC) or 6 h (for BITC and PEITC) at 50 °C the solvent was evaporated. The residue was passed through a short pad of silica gel and the crude product was purified on a silica gel column using hexane/ethyl acetate (7:3) as eluent. The products were fully characterized by multinuclear NMR (^1H, ^{13}C, and ^{15}N) spectroscopy, MS, and elemental analyses. The atom numbering for all three compounds is shown in Fig. 1 and is different from the conventional IUPAC numbering.

N-(1-methylbenzimidazolyl)-N′-allylthiourea ***2a***

Yield 42%; mp 81–82 °C;

UV [λ_{max}, (lg ε), solvent] 344 (4.32), CH_3CN; 340 (2.60), $CHCl_3$;

^1H NMR (DMSO-d_6) δ 3.52, 3.55, 3.78 (3 × s, CH_3, **T1B**, **T1A**, and **T2A**, respectively), 4.00, 4.12, 4.35 (2 × t and br t, $J = 6$ Hz, CH_2NH, **T1A**, **T1B**, and **T2A**, respectively), 5.08 (2 × d, $J = 10$ Hz, $CH = CH_2$ *cis*, **T1A** and **T1B**, respectively), 5.16 (2 × d, $J = 17$ Hz,

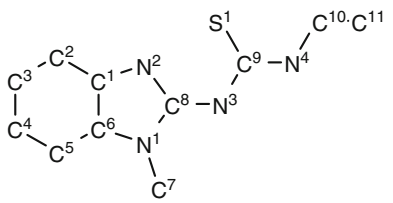

Fig. 1 The numbering of atoms in products **2**

CH=CH_2 *trans*, **T1A** and **T1B**, respectively), 5.20 (d, $J = 10$ Hz, CH=CH_2 *cis*, **T2A**), 5.32 (d, $J = 17$ Hz, CH=CH_2 *trans*, **T2A**), 5.85–5.95 (2 × m, C*H*=CH_2, **T1A** and **T1B**), 5.95–6.06 (m, C*H*=CH_2, **T2A**), 7.15–7.25 (m, 2H, H-3, and H-4), 7.37 (d, $J = 7.7$ Hz, H-5, **T1B**), 7.43 (d, $J = 7.7$ Hz, H-5, **T1A**), 7.46, 7.50 (2 × d, $J = 7.7$ Hz, H-2 and H-5 for **T2A**), 7.55 (d, $J = 7.7$ Hz, H-2, **T1B**), 7.61 (d, $J = 7.7$ Hz, H-2, **T1A**), 8.15 (t, $J = 6$ Hz, N4–H, **T1A**), 8.48 (t, $J = 6$ Hz, N4–H, **T1B**), 10.80 (s, N3–H, **T2A**), 11.60 (t, $J = 6$ Hz, N4–H, **T2A**), 13.10 (s, N2–H, **T1B**), 13.25 (s, N2–H, **T1A**).

^{1}H NMR ($CDCl_3$) δ 3.57, 3.55, 3.70 (2 × s and *br* s, CH_3, **T1B**, **T1A**, and **T2A**, respectively), 4.20, 4.32, 4.48 (2 × t and *br* t, $J = 6$ Hz, CH_2NH, **T1A**, **T1B**, and **T2A**, respectively), 5.18, 5.21 (2 × d, $J = 10$ Hz, CH=CH_2 *cis*, **T1A** and **T1B**, respectively), 5.28, 5.32 (2 × d, $J = 17$ Hz, CH=CH_2 *trans*, **T1A** and **T1B**, respectively), 5.90–6.00 (2 × m, C*H*=CH_2, **T1A** and **T1B**), 6.35 (*br* s, N4–H, **T1A**), 6.60 (*br* s, N4–H, **T1B**), 7.18–7.36 (m, Ar–H, **T1A** and **T1B**), 13.60 (*br* s, N2–H, **T1A** and **T1B**).

There are additional broad peaks in the spectrum centered at 3.70, 4.48, 5.40, and 6.05 ppm that correspond to traces of **T2A** tautomer (about 3–4%);

^{13}C NMR (125.7 MHz, $CDCl_3$): 28.1 (CH_3), 46.5 and 47.0 (NCH_2 for **T1A** and **T1B**, respectively), 108.8 and 109.0 (C5 for **T1B** and **T1A**, respectively), 111.3 and 111.7 (C2 for **T1B** and **T1A**, respectively), 116.8 and 117.0 (C12 for **T1A** and **T1B**, respectively), 123.1, 123.2, and 123.4 (C3/4 for **T1A** and **T1B**), 128.0 (C6), 130.5 (C1), 134.0 and 134.5 (C11 for **T1B** and **T1A**, respectively), 153.8 (C=N), 184.7 (C=S);

IR ν_{max} 3230, 3174, 2989, 2925, 1624, 1612, 1581, 1514, 1479, 1446, 1429, 1402, 1377, 1332, 1315, 1294, 1254, 1242, 1192, 1163, 1144,1126, 1095, 1064, 999, 980, 941, 918, 874, 837, 812, 739, 661, 644, 611, 573 cm^{-1};

MS/MS (*m*/*z*) 247.2 (M + 1), 245.0 (M − 1);

Anal. Calcd. for $C_{12}H_{14}N_4S$: C, 58.51; H, 5.73; N, 22.74; S, 13.02%. Found: C, 58.56; H, 5.73; N, 22.74; S, 13.01%.

N-(1-methylbenzimidazolyl)-N'-benzylthiourea ***2b***

Yield 59%; mp 161–163 °C;

UV [λ_{max}, (lg ε), solvent] 342 (4.98), CH_3CN; 340 (3.55), $CHCl_3$;

^{1}H NMR (DMSO-d_6) δ 3.50, 3.53, 3.78 (3 × s, CH_3, **T1A**, **T1B**, and **T2A**, respectively), 4.59, 4.75, 4.97 (3 × d, $J = 6$ Hz, CH_2NH, **T1A**, **T1B**, and **T2A**, respectively), 7.13–7.60 (m, ArH), 8.55 (t, $J = 6$ Hz, N2–H, **T1A**), 8.85 (t, $J = 6$ Hz, N2–H, **T1B**), 10.80 (s, N3–H, **T2A**), 11.85 (t, $J = 6$ Hz, N4–H, **T2A**), 13.10 (s, N2–H, **T1B**), 13.27 (s, N2–H, **T1A**);

^{15}N NMR (DMSO-d_6, CH_3NO_2) δ −261.0 (N3 for **T2A**), −257.5 (N2 for **T1B**), −256.0 (N2 for **T1A**), −250.5 (N4 for **T2A**), −247.5 (N4 for **T1A**), −245.5 (N4 for **T1B**);

^{1}H NMR ($CDCl_3$) δ 3.58 (s, CH_3, **T1A**), 3.70 (*br* s, CH_3, **T1B**), 4.78 and 4.90 (2 × d, $J = 6$ Hz, CH_2NH, **T1A** and **T1B**, respectively), 6.25 (*br* s, N4–H for **T1B**), 6.60 (t, N4–H for **T1A**), 7.20–7.50 (m, Ar–H), 13.65 (*br* s, N2–H, **T1A** and **T1B**);

^{13}C NMR (125.7 MHz, $CDCl_3$) δ 28.2 (CH_3), 48.0 and 48.5 (NCH_2 for **T1A** and **T1B**, respectively), 109.0 (C5), 111.7 (C2), 123.4 and 123.4 (C3 and C4), 127.5 (C14), 127.7 and 127.8 (C12/16 for **T1B** and **T1A**, respectively), 128.0 (C6), 128.8 and 128.9 (C13/15 for **T1A** and **T1B**, respectively), 130.5 (C1), 138.7 (C11), 153.8 (C=N), 184.7 (C=S);

IR ν_{max}: 3236, 3185, 3072, 3026, 2935, 1622, 1610, 1581, 1529, 1491, 1442, 1400, 1383, 1346, 1308, 1254, 1190, 1153, 1095, 1080, 931, 912, 739, 702, 656, 642, 621, 658, 571 cm^{-1};

MS/MS (*m*/*z*) 297.3 (M + 1), 295.2 (M − 1);

Anal. Calcd. for $C_{16}H_{16}N_4S$: C, 64.84; H, 5.44; N, 18.90; S, 10.82%. Found: C, 64.86; H, 5.45; N, 19.01; S, 10.81%.

N-(1-methylbenzimidazolyl)-N'-phenethylthiourea ***2c***

Yield 63%; mp 141–142 °C;

UV [λ_{max}, (lg ε), solvent] 341 (5.60), CH_3CN; 338 (2.59), $CHCl_3$;

^{1}H NMR (DMSO-d_6) δ 2.88, 2.90, 2.98 (3 × t, $J = 7$ Hz, PhCH_2, **T1A**, **T1B**, and **T1B**), 3.52, 3.59, 3.74 (3 × s, CH_3, **T1B**, **T1A**, and **T2A**), 3.59, 3.70, 3.90 (3 × q, $J = 7$ Hz, NHCH_2, **T1A**, **T1B**, and **T2A**), 7.14–7.62 (m, 9H, Ar–H), 8.10 (t, $J = 6$ Hz, N4–H, **T1A**), 8.42 (t, $J = 6$ Hz, N4–H, **T1B**), 10.70 (s, N4–H, **T2A**), 11.55 (t, $J = 6$ Hz, N3–H, **T2A**), 13.10 (s, N2–H, **T1B**), 13.27 (s, N2–H, **T1A**).

Aliphatic proton signals for **2c** tautomers cannot be assigned unambiguously owing to their nearly equal populations (Table 1).

^{1}H NMR ($CDCl_3$) δ 2.95 and 3.02 (2 × t, $J = 7$ Hz, PhCH_2, **T1A** and **T1B**, respectively), 3.52 and 3.65 (2 × s, CH_3, **T1B** and **T1A**, respectively), 3.80 and 3.95 (2 × q,

Table 1 Solvent-dependent relative population (%) of isomers derived from ^{1}H NMR data for **2** (average results of CH_3, CH_2, and NH proton signals integration; *nd* not detected)

Compound	$CDCl_3$			DMSO-d_6		
	T1A	**T1B**	**T2A**	**T1A**	**T1B**	**T2A**
2a	60	37	3	39	34	27
2b	55	45	nd	43	36	21
2c	55	37	7	35	32	33

$J = 7$ Hz, NHCH_2, **T1A** and **T1B**, respectively), 6.38 (*br* s, N4–H, **T1A**), 6.60 (*br* s, N4–H, **T1B**), 7.18–7.40 (m, 9H, Ar–H), 13.65 (*br* s, N2–H, **T1A** and **T1B**).

There are additional broad peaks in the spectrum centered at 3.10 and 4.08 ppm that correspond to traces of **T2A** tautomer (about 7%);

^{13}C NMR (125.7 MHz, $CDCl_3$) δ 28.2 (CH_3), 35.3 and 35.9 (CH_2Ph, **T1B** and **T1A**, respectively), 45.3 and 45.5 (NCH_2, **T1A** and **T1B**, respectively), 108.7 and 109.0 (C5, **T1B** and **T1A**, respectively), 111.3 and 111.7 (C2, **T1B** and **T1A**, respectively), 123.0, 123.2, and 123.4 (C3/4, for **T1B** and **T1A**, respectively), 126.7 (C15), 128.0 (C6), 128.8, 128.9, 129.0, and 129.1 (C13/17 and C14/16, **T1A** and **T1B**), 130.5 (C1), 139.3 (C11), 153.8 (C=N), 184.7 (C=S);

IR ν_{max} 3296, 3186, 3062, 3026, 2935, 1622, 1614, 1595, 1479, 1446, 1402, 1373, 1350, 1322, 1286, 1246, 1149, 1128, 1093, 1064, 999, 933, 742, 698, 661, 634, 617, 573 cm^{-1};

MS/MS (*m*/*z*) 311.1 (M + 1), 309.2 (M − 1);

Anal. Calcd. for $C_{17}H_{18}N_4S$: C, 65.78; H, 5.84; N, 18.05; S, 10.33%. Found: C, 65.93; H, 5.90; N, 17.81; S, 10.23%.

Results and discussion

Synthesis

The efficient synthesis of the respective thioureas **2** appears to be simple, but the MABI–aliphatic ITC system was expected to exhibit low reactivity. The mechanism of aminolysis was studied in detail only for aromatic ITCs [14]. MABI is a base about 10^3 times weaker than typical aliphatic amines, and aliphatic ITCs are less reactive than aryl ITCs (owing to the lack of the crucial negative resonance effect of the phenyl ring). Deprotonation considerably enhances the nucleophilicity of **1**, but in this case the formation of double addition byproducts would be preferred, as shown, e.g., for the structurally related 2-amino-1-methyl-5-nitroimidazoles [15].

The synthesis of the target 1-benzimidazolylthioureas **2** was carried out after the optimization of reaction conditions based on the model reaction between **1** and PEITC leading to **2c**. The effect of solvent, stoichiometry, concentration, temperature, and base on the course of the above reaction was studied.

We tested various solvents (iPrOH, EtOH, MeOH, THF, DMF), but the best results were obtained when the reaction took place in MeCN. Neither the reagent ratio (using **1** or ITC in two-fold excess), nor longer reaction times, nor a higher temperature pushed the reaction to completion. In all runs, there was always some unreacted **1** or ITC present in the reaction mixture. The yields (42–63%) are the mean values of at least three experiments and correspond to the amounts of products isolated following chromatographic purification. Although the target thioureas **2** were obtained only in moderate yields, these results are quite similar to those achieved during aminolysis of aliphatic ITC with various 2-amino substituted nitrogen heterocycles [4, 16]. The reason why the reaction tends to stop at moderate conversion even after a prolonged reaction time (>3 days) is not understood at the present time.

NMR analysis

According to a previous report [9], PITC adducts **2d** and **2e** in $CDCl_3$ and DMSO solutions at room temperature adopt one tautomeric form only. On the basis of NMR analysis, we concluded that adducts **2a**–**c** consist of a mixture of at least three isomers in both solutions. At first sight, ^{1}H NMR spectra of chloroformic solutions of **2** contained only two sets of well-resolved resonances for each CH proton and three signals of exchangeable NH protons. However, careful NMR analysis revealed the presence of additional broad peaks (4–7%) resulting from a dynamic process between two additional isomers. Also, for spectra recorded in DMSO, all CH triplicate signals and six sharp peaks of exchangeable NH protons were observed, indicating the presence of three isomers for **2a**, **2b**, and **2c**.

If we consider only the partial double bond character of four C–N bonds (N2–C8, C8–N3, N3–C9, and C9–N4), there are up to eight possible isomers of **2**. In contrast, the presence of four adjacent basic sites—three on a nitrogen atom and one on a sulfur atom with two acidic protons—suggests the possible existence of additional tautomers. It is well known that ZE isomers of unsymmetrically disubstituted thioureas are more stable than the respective ZZ/EE isomers, and isomers able to form strong intramolecular bonding are preferred over others [17].

It should be mentioned that an enaminethiol form of thiourea derivatives has never been detected in the ground state because of its extremely low population in the equilibrium state. However, a few years ago, Nowak detected an unstable enaminethiol tautomer of thiourea in a cryogenic argon matrix after UV irradiation [18]. Among the trial structures, we selected the most probable isomers that satisfy the above conditions; some of them are presented in Fig. 2.

As mentioned above, three NH proton signals appeared in $CDCl_3$ solutions, one about 14 ppm and two at a lower frequency (6–7 ppm). It is well known that the NH signal observed at a higher frequency is of intermolecular H-bond origin (chelated) and thus corresponds to the structures **T1A**, **T1B**, or **T2A**. A small difference in the chemical

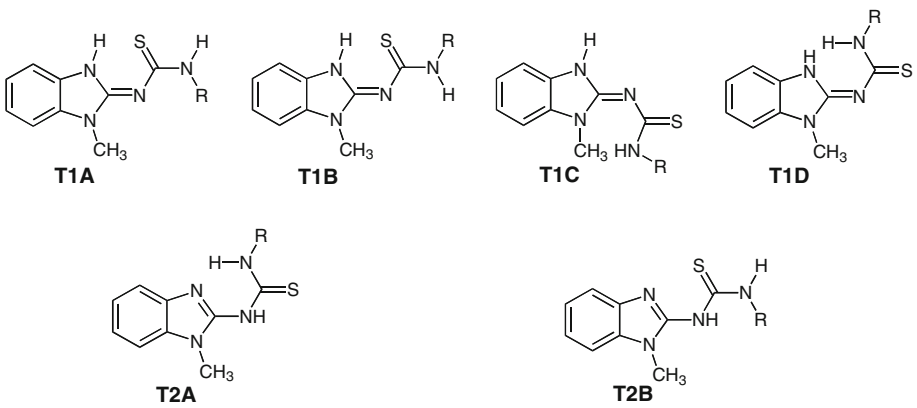

Fig. 2 The most plausible isomers of adducts **2**. Structures **T1C** and **T2B** are excluded due to either lack of chelated protons or NOE correlations (see text for explanation)

shifts of both non-chelated NH protons ($\Delta\delta = 0.5$ ppm) suggests a structural similarity between these two tautomers; they are denoted by **T1A** and **T1B**.

The observed multiplicity of N(4)H proton signals (triplets) enabled differentiation of the respective signals in every ^{1}H NMR spectrum recorded in DMSO (Fig. 3).

Both NH proton peaks of **T2A** tautomers occurred between the N(2)H and N(4)H proton peaks of **T1A** and **T1B**. The N(4)H proton in **T2A** was always more deshielded (about 12 ppm) than the N(3)H proton (about 11 ppm). For tautomers **T1B** and **T2A**, the trend was reversed. The N(2)H protons in all **2** were the most deshielded (δ 13.2 and 13.1 ppm for **T1A** and **T1B**, respectively). Otherwise, the N(4)H proton signals lie about 4 ppm upfield (δ 8.0 and 8.2 for **T1A** and **T1B**, respectively). This means that the N(4)H proton in **T2A** has a significantly different surrounding and that its increased deshielding, compared to the corresponding signals for **T1A** and **T1B** ($\Delta\delta \sim 4$ ppm), is an effect of intramolecular hydrogen bonding.

An interesting feature was observed for CH protons. The chemical shift measured in DMSO-d_6 decreases in the following order: **T1A** < **T1B** < **T2A** (for NCH_2 protons) and **T1A** ~ **T1B** < **T2A** (for CH_3 protons). The last sequence indicates again (see above) that **T2A** tautomers differ significantly in structure from both **T1A** and **T1B**, mainly in the benzimidazolyl fragment. The following important information was extracted from our ROESY experiments. We found significant NOE effects that unambiguously indicated the orientation of the main structural units of **2**. Therefore, N–CH_3 protons in **T1A** correlate with N(4)CH_2 protons while N–CH_3 protons in **T2A** correlate with the N(3)H proton. The lack of NOEs for N–CH_3 and N(4)H means that the postulated structure **T1C** for the main tautomer can be ruled out. The correlated ^{1}H–^{15}N gHSQC spectrum of **2b** in DMSO makes it possible to distinguish between all the tautomers detected. It was found that the N4 nitrogens for all three tautomers are more deshielded than the N2/N3 ones ($\Delta\delta = 8.5$–12 ppm). For **T1A** and **T1B** tautomers, the N2 and N4 signals are close to each other, but for **T2A** both signals appear at a higher field (3.5–5 ppm).

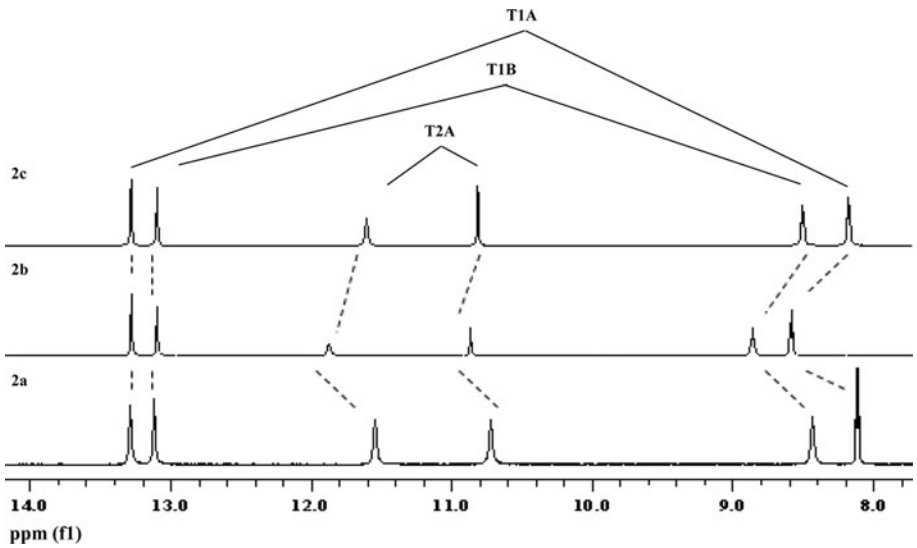

Fig. 3 ^{1}H NMR spectra of **2** in DMSO-d_6

The main conclusion is that the reported chemical shifts confirm that the N2 nitrogens in **T1A** and **T1B**, as well as the N3 nitrogen in **T2A** are all sp^3-hybridized.

Additional valuable information can be derived from ^{13}C NMR spectra. The observed significant shielding (referenced to **1**) of C1 tertiary carbon ($\Delta\delta_{\mathbf{2-1}} = -11.4$ ppm), together with the shielding of the aromatic C2 carbon ($\Delta\delta_{\mathbf{2-1}} = -3.4$ ppm), reveal once again that N2 is sp^3-hybridized, which is an additional proof for the proposed structures of both **T1A** and **T1B** tautomers. Interestingly, all the **T1B** signals in ^{13}C NMR spectra recorded in chloroform are broad and not always detectable. Broadening of the respective signals for **T1B** and **T2A** in their ^1H NMR spectra may indicate a relationship between **T1B** and **T2A** and their possible interconversion. The mechanism of such an interconversion remains an unsolved problem. On the other hand, the conversion of **T1A** to **T1B** appears to proceed because of the restricted rotation about the C9–N4 bond.

It should be mentioned that the ^1H NMR spectrum of **2b** recorded immediately after its dissolution in DMSO contained only **T1A** and **T1B** signals; signals of **T2A** arose slowly over time.

The thiocarbonyl C=S chemical shift of 184.7 ppm (the same for all **2**) is different from that of other unsymmetrical thioureas containing alkyl and heteroaryl residues ($\delta = 176$–181 ppm) [4, 16]. This extra deshielding is caused by the partial ionic character of the C=S bond (vide infra the observed C–S bond length in crystal).

In our hands, the most accurate method for determining the **2a**–**2c** tautomer ratio was ^1H NMR spectroscopy. In DMSO, the observed exchange reactions are slow enough to see all NH protons as sharp isolated signals, which make the populations of all three tautomers easily measurable. The results obtained for NH, as well as for CH protons were found to be comparable. However, this approach cannot be used for **2c**, where the populations of all three tautomers are comparable (Table 1).

IR analysis

ATR spectra in the characteristic 2500–4000 cm^{-1} range of compounds **2** are displayed in Fig. 4. In the higher wavenumber region, 3100–3300 cm^{-1}, there are several bands that are characteristic of the asymmetric and symmetric stretching vibrations of the NH bonds involved in the formation of intra- and intermolecular hydrogen bonds in the crystals. The shift of the ν(N–H) band of **2c** toward higher wavenumbers (ca. 3300 cm^{-1}) may suggest that the hydrogen bonds involved in dimer formation in crystals are weaker than in the case of **2a** and **2b** [19].

The bands in the 739–742 cm^{-1} region are characteristic of ν(C=S), and the absence of S–H stretching vibrations at ca. 2550 cm^{-1} indicates that the compounds in the solid state remain as a thione tautomer [20].

The absorptions observed at 1479–1491 cm^{-1} [21] and 1093–1095 cm^{-1} ranges correspond to N–C–N stretching vibrations in thioureas. The increase in frequency in relation to the thioureas described in the literature [22] can be attributed to the greater double bond character of the C–N bond in products **2**.

X-ray structure analysis

The general and crystallographic data for compounds **2a**, **2b**, and **2c** are listed in Table 2. The numbering of atoms in products **2** is shown in Fig. 1. The main geometrical features of the structures of these compounds are given in Table 3. All the data in Tables 3, 4, 5 are compared to the parameters of the published previously *N*-(2-phenoxyethyl)benzimidazolyl-*N*′-phenethylthiourea **2e** [9]. Only one isomer is observed in the crystals of **2a**–**2c**, and its structure corresponds to one of those (namely **T1A**) deduced from NMR analysis. Therefore, **T1A** predominates in all the compounds under investigation in the solid state and in solution. It forms centrosymmetric dimers in all cases.

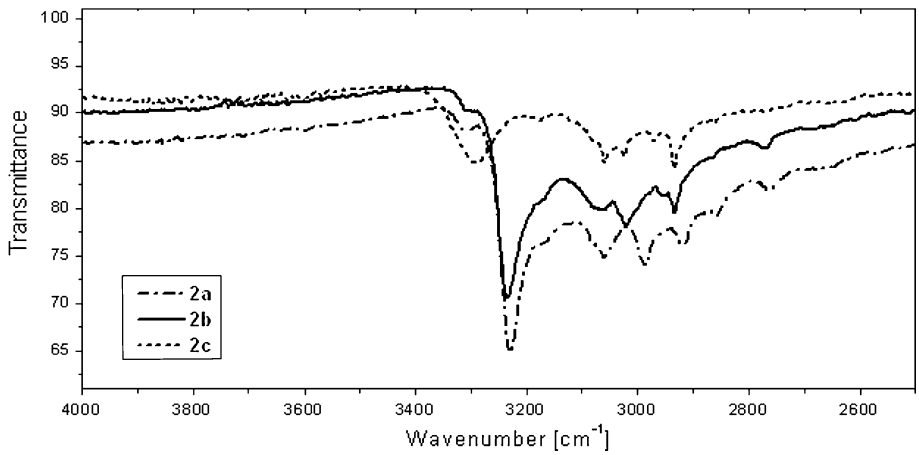

Fig. 4 ATR spectra of products **2** in the crystalline state in the 4000–2500 cm^{-1} range

Table 2 Summary of crystal data, intensity collection, and structure refinement for compounds **2a**, **2b**, and **2c**

Compounds	**2a**	**2b**	**2c**
Code	CCDC 751508	CCDC 752764	CCDC 751509
Crystal color and habit	Yellow prism	Yellow prism	Colorless prism
Empirical formula	$C_{12}H_{14}N_4S_1$	$C_{16}H_{15}N_4S_1$	$C_{17}H_{18}N_4S_1$
M_r	246.33	296.39	310.41
Temperature (K)	120(2)	120(2)	120(2)
Wavelength (Å)	0.71073	0.71073	0.71073
Crystal system, space group	Triclinic, $P\bar{1}$	Triclinic, $P\bar{1}$	Triclinic, $P\bar{1}$
Unit cell parameters			
a (Å)	9.672(3)	9.1003(5)	9.6509(9)
b (Å)	7.541(3)	9.1926(5)	9.7089(13)
c (Å)	9.267(3)	10.2034(4)	10.3757(17)
α (°)	90.39(3)	89.760(4)	65.086(14)
β (°)	111.58(3)	82.410(4)	64.455(12)
γ (°)	104.63(3)	60.603(5)	79.705(9)
Cell volume (Å^3)	604.5(4)	735.33(6)	795.5(2)
Z	2	2	2
Density (g cm^{-3})	1.353	1.339	1.296
Absorption coefficient (mm^{-1})	0.251	0.219	0.205
F(000)	260	312	328

Table 3 Selected bond lengths (Å) for **2a**–**2c** and **2e** (taken from ref. [9])

Compound	C9–S1	C9–N3	C9–N4	C8–N3	C8–N2	C8–N1	N1–C7	N4–C10
2a	1.724(2)	1.343(2)	1.340(2)	1.322(2)	1.361(2)	1.362(2)	1.457(2)	1.462(2)
2b	1.726(2)	1.348(2)	1.344(2)	1.325(2)	1.360(2)	1.361(2)	1.457(2)	1.464(2)
2c	1.721(2)	1.349(2)	1.341(2)	1.327(2)	1.354(2)	1.364(2)	1.455(2)	1.456(2)
2e	1.725(1)	1.341(2)	1.364(2)	1.335(2)	1.350(2)	1.367(2)	1.458(2)	1.417(2)

Table 4 Selected interatomic distances (Å), valence, torsion, and dihedral angles (°) for **2a**–**2c** and for **2e** (taken from ref. [9])

Compound	Intramolecular hydrogen bond parameters			Dihedral angles		Torsion angles	
	N(2)H···S(1)	N(2)···S(1)	∠N(2)HS	∠($P1$, $P2$)	∠($P1$, $P3$)	θ_1	θ_2
2a	2.352	2.990	130	4.1	47.4	−1.8	177.4
2b	2.356	2.984	131	5.6	139.2	−1.6	177.4
2c	2.315	2.975	131	13.3	66.5	−8.3	169.2
2e	2.287	2.946	133	5.3	7.0	−0.5	179.9

θ_1 = C8–N3–C9–S1; θ_2 = S1–C9–N4–C10; $P1$ = benzimidazolyl ring, $P2$ = thiourea plane, $P3$ = phenyl ring or ethene plane

The crystal structures described here resemble the ones previously reported for analogous *N*-substituted derivatives of **1** and PITC (**2e**). However, the C9–N4 bond in **2a**, **2b**, and **2c** is shorter than in **2e** because of the direct N4 atom bonding to the aromatic ring (phenyl) instead of alkyl carbon. Typically, the C=S bond length is 1.60 Å [23], but the C9–S1 bond in all thioureas **2** under investigation undergoes resonance lengthening (1.72 Å). The fact that the benzimidazole ring is nearly coplanar with the thiourea core (see Table 4) indicates that there is a significant contribution of the respective resonance forms for **2a** and **2b**. Otherwise, there is a remarkable distortion of molecule of **2c** manifested in the large dihedral angle between benzimidazolyl ring and thiourea plane ($P1$ and $P2$) (13.3°) and deviation from planarity in the thiourea core (θ_1 and θ_2: –8.3 and 169.2°). Despite the smallest interplanar distance between thiourea planes $P2$–$P2'$ in the hydrogen bond linked dimeric system (0.16 Å, almost flat dimer) and shorter H···S distance found for **2c**, it could not form an intermolecular hydrogen bonding network that was

Table 5 Intermolecular hydrogen bonds and π–π stacking parameters (°, Å) for dimeric **2a**–**2c** and for **2e** (taken from ref. [9])

Compound	∠N(2)HS′	N(2)H···S(1)′	N(2)···S(1)′	Interplanar distance *P2*–*P2*′ in dimers	Shortest centroid-to-centroid distances
2a	167.0	2.565	3.379	1.05	4.153(2) (Imid → Imid')
2b	161.4	2.596	3.407	0.33	3.905(2) (Imid → Benz) 4.023(2) (Ph → Ph)
2c	166.9	2.546	3.399	0.16	4.443(2) (Imid → Benz)
2e	163.5	2.627	3.466	0.60	–

Prime denotes the symmetry equivalent atom or group (by inversion). Imid: ring C1–N2–C8–N1–C6, Benz: ring C1–C6, Ph: C11–C16

stronger than in **2a** and **2b**. It could be explained by the loss of more energy for conformation change required to form the dimer (see text below and Fig. 9). As mentioned above, ATR results confirmed that the N–H stretching vibration band for **2c** is shifted to the left (about 100 cm^{-1}), which indicates weaker intramolecular bondings in its dimers.

On the other hand, the strength of the connections between dimers in **2c** is smaller than the respective interactions between **2a** and **2b** dimers (Figs. 5, 6, 7). The lack of π–π stacking interactions (see Table 5; for comparison: interplanar distance in graphite is 3.35 Å) or other relevant bonding contacts induces larger distances between dimers in chains and between parallel chains. As expected, the crystal of **2c** has the lowest density, too.

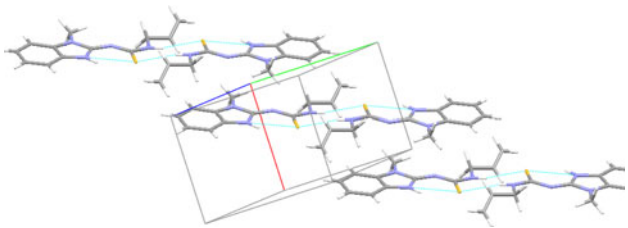

Fig. 5 Crystal packing in **2a**. Thiourea dimers held together by weak π–π stacking of the Imid–Imid rings

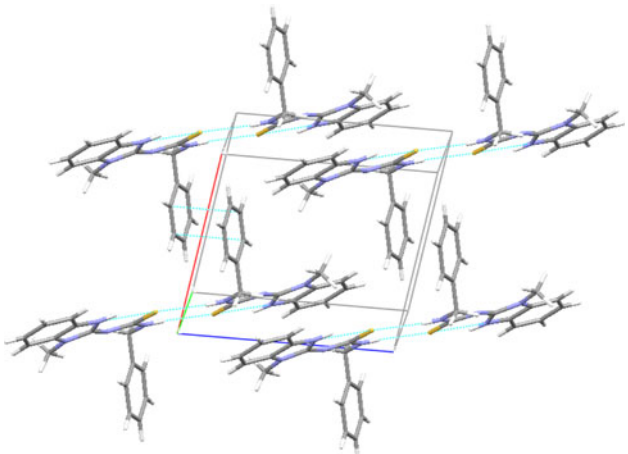

Fig. 6 Crystal packing in **2b**. Two π–π stackings (between Imid–Benz and Ph–Ph rings) bind thiourea dimers

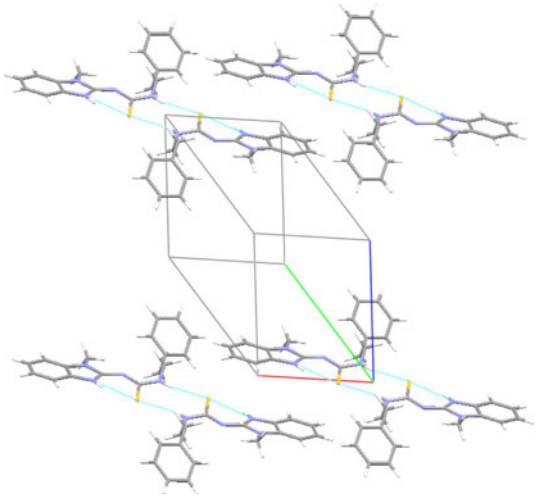

Fig. 7 Crystal packing in **2c**. Thiourea dimers held together by weak π–π stacking (Imid–Benz rings)

Table 6 Relative energies (B3LYP/6-311+G(d,p)//B3LYP/6-31G(d,p), ZPE corrected, kcal/mole) calculated for isomers of **2**

Compound	**T1A**	**T1B**	**T2A**
2a	0	−0.64	+2.89
2b	0	−0.94	+2.97
2c	0	−0.90	+2.19
2d (EtOH)	0	Not reported	+5.0

Isomer **T1B** is a rotamer of **T1A**, while **T2A** is a tautomer of **T1A**

Calculations

To confirm the identity of the tautomers present in solution, DFT calculations of optimized geometries were carried out on **2** (Table 6). It was found for **2b** and **2c** that in the gas phase, the energies of **T1A** tautomers are significantly lower than those of **T2A** tautomers. Isomers **T2A** of **2a**, **2b**, and **2c** are less stable with relative energies of +2.89, +2.97, and +2.19 kcal/mole, respectively. These values are smaller than previously reported for **2d** (+5.0 kcal/mole) in ethanol [9]. This could lead to measurable coexisting populations of all isomers of **2a–c** in solution after taking into account the extra stabilization of **T2A** by DMSO.

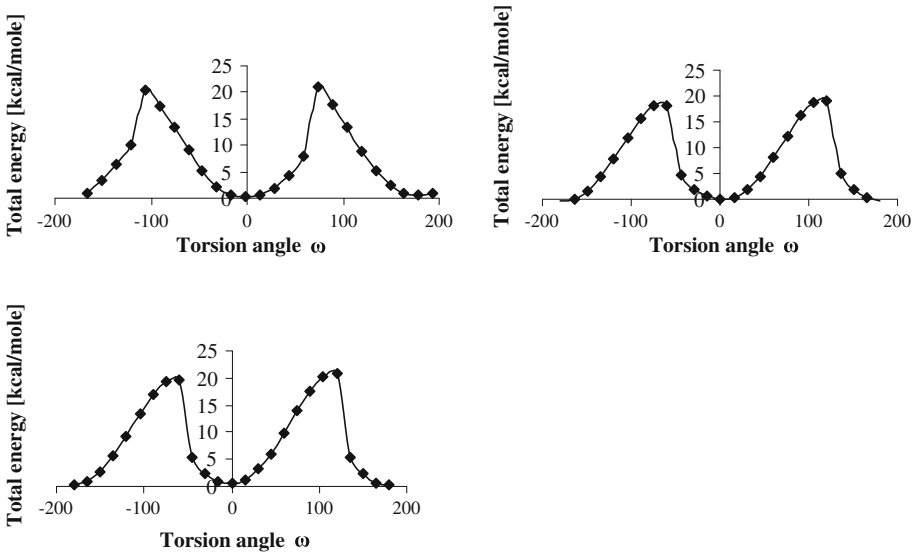

Fig. 8 Relaxed potential energy scan (B3LYP/6-31G(d,p)) for rotation about the C9–N4 bond for **2a** (*left*), **2b** (*right*), and **2c** (*below*). The scan coordinate is the torsion angle H–N4–C9–S1; other geometrical parameters were allowed to optimize. The different slopes on the left and right sides of the curves stem from the transition from sp^2 to sp^3 hybridization mode at the nitrogen atom during rotation. Rotational barriers for **2a**, **2b**, and **2c** can be estimated as 18.1, 18.8, and 19.9 kcal/mole, respectively

Surprisingly, the calculations revealed that the energy of **T1A** is slightly higher than that of **T1B** in isolated molecules (note: the formation of dimers can reverse the energy preferences). Therefore, **T1B**, not **T1A** is the lowest-energy tautomer for **2a**, **2b**, and **2c**.

Another unexpected feature of thioureas **2** is the unusually high rotational barrier about the C9–N4 bond (based on B3LYP/6-31G(d,p) PES scan). Both calculated energies are up to 7–9 kcal/mole higher than those determined experimentally for 1,3-dialkyl thioureas [24]. Since it is well known that the respective theoretical values for thioureas are usually 3–4 kcal/mole smaller [25], actual energy barriers in DMSO should be even higher than predicted theoretically for isolated molecules. The calculations also showed that mutual interconversion **T1A**⇆**T1B** requires about 2 kcal/mole more energy in the case of **2c** than **2b** (Fig. 8).

Overlays of experimental and calculated structures of **T1A** are presented in Fig. 9. Clearly, formation of the dimers can induce conformational changes in the molecules. This effect is more marked for **2c**.

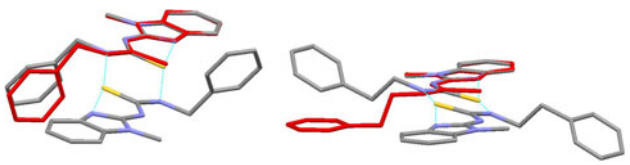

Fig. 9 The overlay of X-ray and calculated (*red*) structures of **2b** (*left*), and **2c** (*right*). The hydrogen bond network is additionally shown for the crystal structures. The benzimidazole residue was chosen as the basis for fitting. (Color figure online)

Conclusion

Crystallographic results regarding the structures of 2-benzimidazolylthiourea **2** adducts of aliphatic ITCs and MABI confirm that in the solid state their only form is the tautomer **T1A**, existing as the **T1A**–**T1A** centrosymmetric dimer, as found previously for the respective adducts of PITC [9]. The data presented here provide spectroscopic evidence that the intramolecular hydrogen bonds observed in the solid state are also maintained in DMSO solution for the main isomer **T1A**.

Being typical unsymmetrical thioureas, **2** are bonded into dimers through double intermolecular NH···S bonds. *N*-Substituents in **2** strongly affected contacts and the strength of H-bonding was indicated by comparison of the respective structural parameters. Otherwise, in solution, **2** exists as a mixture of three tautomers. In chloroform, **T1A** is clearly dominant over **T1B** and **T2A**, whereas in DMSO all three isomers exist in nearly equal proportions. The structures of all tautomers were predicted theoretically and unequivocally elucidated experimentally. It was quite surprising to find unusual NOE interactions for **T1A** in solution. This provides additional proof for the enhanced double bond nature of N4–C9 in **2**, which makes them more rigid and also strengthens the intermolecular bonding in their dimers.

The structure of **T1A** corresponds to that found in crystal; on dissolving in DMSO, thiourea dimers **T1A**–**T1A** start to dissociate slowly. As a result of rotation about the C9–N4 bond, **T1A** is transformed into isomer **T1B** (nearly equal in energy according to calculations). It cannot form dimers because of the opposing positions of the C=S acceptor group and the N(4)H donor. The calculated barrier to rotation about the C9–N4 bond is equal to ca. 18–20 kcal/mole for all thioureas **2**. During dissolution,

rotation about the N3–C9 bond yielded the rotamer **T1D** as a precursor of tautomer **T2A.** Tautomers **T2A** arise as a result of proton transfer from nitrogen N(2) to N(3) and are higher energy isomers (about 3 kcal/mole). **T2A** is not able to form dimers either.

We conclude that DMSO as a solvent balances the energy differences between all the isomers with the special stabilization of **T2A**, the most polar one in solution. Our results, obtained from NMR and crystallographic data, are corroborated by theoretical calculations.

This is the first report of three isomers of unsymmetrical thioureas existing in equilibrium with an exchange rate at room temperature that is sufficiently slow to permit the unambiguous resolution of their structures. Due to the fact that analogous **2d** exists as one isomer at room temperature, we claim that the observed different behaviors of thioureas **2a–c** are their unique feature. Therefore, the statement that 2-benzimidazolylthioureas exist exclusively as one 1,3-dihydrobenzimidazolinylidene tautomer [9] is not general and should be reserved only for the relevant *N*′-phenylthioureas.

Acknowledgments The studies were supported by the Polish Ministry of Science and Higher Education, grant No. 312244336 and by the European Union (European Social Fund) within the framework of the project "InnoDoktorant—Scholarships for PhD students, 1st edition." Calculations were carried out at the Academic Computer Center in Gdansk (TASK).

References

1. Mukerjee AK, Ashare R (1991) Chem Rev 91:1–24
2. de Dios A, Shih C, López de Uralde B, Sánchez C, del Prado M, Cabrejas LMM, Pleite S, Blanco-Urgoiti J, Lorite MJ, Nevill CRJ, Bonjouklian R, York J, Vieth M, Wang Y, Magnus N, Campbell RM, Anderson BD, McCann DJ, Giera DD, Lee PA, Schultz RM, Li LC, Johnson LM, Wolos JA (2005) J Med Chem 48:2270–2273
3. Saedd S, Rashid N, Jones PG, Ali M, Hussain R (2010) Eur J Med Chem 45:1323–1331
4. Tsogoeva SB, Hateley MJ, Yalalov DA, Meindl K, Weckbecker C, Huthmacher K (2005) Bioorg Med Chem 13:5680–5685
5. Gunnlaugsson T, Glynn M, Tocci GM, Kruger PE, Pfeffer FM (2006) Coord Chem Rev 250:3094–3117
6. Zhang Y-M, Cao Ch, Wei W, Xie T-B (2007) Chin J Chem 25:709–713
7. Lee GW, Singh N, Jank DO (2008) Tetrahedron Lett 49:1952–1956
8. Succaw GL, Weakley TJR, Han F, Doxsee KM (2005) Cryst Growth Des 5(6):2288–2298
9. Morkovnik AS, Divaeva LN, Nelyubina YV, Lyssenko KA, Vasilchenko IS (2007) Mendeleev Commun 17:224–226
10. Oxford Diffraction Ltd, Abingdon, England (2006) CrysAlis CCD, CrysAlis RED and associated programs. Oxford Diffraction Ltd, Abingdon, England
11. Sheldrick GM (2008) Acta Cryst A64:112–122
12. Macrae CF, Bruno IJ, Chisholm JA, Edgington PR, McCabe P, Pidcock E, Rodriguez-Monge L, Taylor R, van de Streek J, Wood PA (2008) J Appl Cryst 41:466–470
13. Frisch MJ, Trucks GW, Schlegel HB, Scuseria GE, Robb MA, Cheeseman JR, Montgomery Jr JA, Vreven T, Kudin KN, Burant JC, Millam JM, Iyengar SS, Tomasi J, Barone V, Mennucci B, Cossi M, Scalmani G, Rega N, Petersson GA, Nakatsuji H, Hada M, Ehara M, Toyota K, Fukuda R, Hasegawa J, Ishida M, Nakajima T, Honda Y, Kitao O, Nakai H, Klene M, Li X, Knox JE, Hratchian H P, Cross JB, Bakken V, Adamo C, Jaramillo J, Gomperts R, Stratmann RE, Yazyev O, Austin AJ, Cammi R, Pomelli C, Ochterski JW, Ayala PY, Morokuma K, Voth GA, Salvador P, Dannenberg JJ, Zakrzewski VG, Dapprich S, Daniels AD, Strain MC, Farkas O, Malick DK, Rabuck AD, Raghavachari K, Foresman JB, Ortiz JV, Cui Q, Baboul AG, Clifford S, Cioslowski J, Stefanov BB, Liu G, Liashenko A, Piskorz P, Komaromi I, Martin RL, Fox DJ, Keith T, Al-Laham MA, Peng CY, Nanayakkara A, Challacombe M, Gill PMW, Johnson B, Chen, W, Wong MW, Gonzalez C, Pople JA (2004) Gaussian 03, revision D.01. Gaussian, Inc., Wallingford, CT
14. Satchell DPN, Satchell RSJ (1990) Chem Soc Perkin Trans 2:1415–1420
15. Sudarsanam V, Nagarajan K, Arya VP, Kaulgud AP, Shenoy SJ, Shah RK (1982) Indian J Chem 21B:989–996
16. Saxena A, Pike RD (2007) J Chem Crystallogr 37:755–764
17. Sudha LV, Sathyanarayana DN (1984) J Mol Struct 40:751–755
18. Rostkowska H, Lipiński L, Khvorostov A, Nowak MJ (2003) J Phys Chem A 107:6373–6380
19. Marechal Y (2007) The hydrogen bond and the water molecule. Elsevier, Amsterdam, pp 85–89
20. Weiqun Z, Wen Y, Lihu Q, Yong Z, Zhengfenh Y (2005) J Mol Struct 749:89–95
21. Kirubavathi K, Selvaraju K, Kumararaman S (2008) Spectrochim Acta A 71:1–4
22. Kirubavathi K, Selvaraju K, Valluvan R, Kumararaman S (2007) Mater Lett 61:4173–4176
23. Borjesson K, Sandin P, Wilhelmsson LM (2009) Biophys Chem 139(1):24–28
24. Sullivan RH, Price E (1975) Org Magn Reson 7:143–150
25. Haushalter KA, Lau J, Roberts JD (1996) J Am Chem Soc 118:8891–8896